Operational Equilibria of Electric and Natural Gas Systems with Limited Information Interchange

Sheng Chen, *Member, IEEE,* Antonio J. Conejo, *Fellow, IEEE,* Ramteen Sioshansi, *Senior Member, IEEE,* and Zhinong Wei

***Abstract*—Electric power and natural gas systems are typically operated independently. However, their operations are interrelated due to the proliferation of natural gas-fired generating units. We analyze the independent but interrelated day-ahead operation of the two systems. We use a direct approach to identify operational equilibria involving these two systems, in which the Karush-Kuhn-Tucker conditions of both electric power and natural gas operational models are gathered and solved jointly. We characterize the equilibria that are obtained under different levels of temporal and spatial granularity in conveying information between the two system operators. Numerical results from the Belgian system are used to examine the impacts of different levels of information interchange on prices, operational costs, decisions in the two systems.**

***Index Terms*—Power system operations, natural gas, locational marginal pricing, complementarity modeling**

NOMENCLATURE

Indices, Sets, and Functions

$\mathbb{C}(m)$	set of natural gas compressors connected to node m
$\mathbb{E}(i)$	set of buses directly connected to bus i
$\mathbb{G}(m)$	set of nodes directly connected to node m
i, j	indices of electric buses in set, $\mathbb{B}$
k	index of natural gas compressors
m, n	indices of natural gas nodes in set, $\mathbb{N}$
REF	reference bus
t	time index in set, T
v	index of generating units
w	index of natural gas suppliers
Θ_i^G	set of generating units connected to bus i
Ψ_m^G	set of natural gas-fired units connected to node m
Ψ_m^S	set of natural gas suppliers connected to node m
Ω_G	set of natural gas-fired generating units
Ω_R	set of non-natural gas-fired generating units

Parameters and Constants

C^E	value of lost electric load [\$/p.u.]
C^G	value of lost natural gas load [\$/Mm^3]
$C_{G,v}$	variable production cost of non-natural gas-fired generating unit v [\$/p.u.]
$C_{O,v}$	non-fuel variable operation and maintenance cost of natural gas-fired unit v [\$/p.u.]
$C_{S,w}$	variable production cost of natural gas supplier w [\$/Mm^3]
$F_{C,k}^{\max}$	natural gas-transportation limit of compressor k [Mm^3/h]
$F_{L,m,t}$	hour-t non-generation-related natural gas demand at node m [Mm^3/h]
$F_{S,w}^{\max}$	capacity of natural gas supplier w [Mm^3/h]
$F_{S,w}^{\min}$	minimum natural gas supply from supplier w [Mm^3/h]
$F_{S,w}^{\text{ramp}}$	ramping limit of natural gas supplier w [Mm^3/h]
$K_{m,n}$	line-pack parameter of pipeline connecting nodes m and n [Mm^3/bar]
$L_{\min}$	minimum total line-pack in the natural gas system [Mm^3]
$P_{G,v}^{\max}$	capacity of generating unit v [p.u.]
$P_{G,v}^{\min}$	minimum power output of generating unit v [p.u.]
$P_{G,v}^{\text{ramp}}$	ramping limit of generating unit v [p.u./h]
$P_{i,j}^{\max}$	capacity of the line connecting buses i and j [p.u.]
$P_{L,i,t}$	hour-t electric demand at bus i [p.u.]
$W_{m,n}$	Weymouth constant of the pipeline connecting nodes m and n [(Mm^3/h)/bar]
$\zeta_{m,t}$	hour-t price of natural gas at node n [\$/Mm^3/h]
η_v	heat rate of natural gas-fired unit v [Mm^3/h/p.u.]
ϑ_k	conversion efficiency of gas compressor k [p.u.]
$\pi_m^{\max}$	maximum node-m natural gas pressure [bar]
$\pi_m^{\min}$	minimum node-m natural gas pressure [bar]
$\rho_k^{\max}$	maximum compression ratio of compressor k [p.u.]
$\rho_k^{\min}$	minimum compression ratio of compressor k [p.u.]
$\sigma_{i,j}$	susceptance of line connecting buses i and j [p.u.]

Variables

$F_{C,k,t}$	hour-t natural gas flow through compressor k [Mm^3/h]
$F_{L,m,t}^D$	non-generation-related natural gas demand at node m that is served in hour t [Mm^3/h]
$F_{m,n,t}$	hour-t natural gas flow through the pipeline connecting nodes m and n [Mm^3/h]
$\bar{F}_{m,n,t}$	average hour-t natural gas flow through the pipeline connecting nodes m and n [Mm^3/h]
$F_{S,w,t}$	natural gas supplied in hour t by supplier w [Mm^3/h]
$L_{m,n,t}$	hour-t line-pack in the pipeline connecting nodes m and n [Mm^3/h]
$P_{G,v,t}$	hour-t active power output from generating unit v [p.u.]
$P_{L,i,t}^D$	bus-i electric demand that is served in hour t [p.u.]

This work was supported by National Natural Science Foundation of China grant 51877071 and National Science Foundation grant 1808169.

S. Chen and Z. Wei are with the College of Energy and Electrical Engineering, Hohai University, Nanjing 210098, China (e-mail: chenshenghhu@163.com; wzn_nj@263.net).

A. J. Conejo is with the Department of Integrated Systems Engineering and the Department of Electrical and Computer Engineering, The Ohio State University, Columbus, OH 43210, USA (e-mail: conejo.1@osu.edu).

R. Sioshansi is with the Department of Integrated Systems Engineering, The Ohio State University, Columbus, OH 43210, USA (e-mail: sioshansi.1@osu.edu).

$\theta_{i,t}$ hour-t phase angle of bus i [rad]
$\pi^{\text{in}}_{k,t}$ hour-t inlet pressure of compressor k [bar]
$\pi^{\text{out}}_{k,t}$ hour-t outlet pressure of compressor k [bar]
$\pi_{m,t}$ hour-t natural gas pressure at node m [bar]
$\tau_{k,t}$ hour-t natural gas consumption of compressor k [Mm^3/h]

I. Introduction

PROLIFERATION of natural gas-fired generating units is increasing the coupling of electric power and natural gas systems [1], [2]. Despite this coupling, these systems are typically planned and operated independently of one another, which may be sub-optimal [3]–[5]. This issue may be addressed using a joint operational model that yields an optimal solution for both systems [6]. There are, however, non-trivial institutional and administrative barriers to having a single entity operate both systems. Thus, it may be preferable to independently operate the two systems, while having some form of co-ordination between them.

The existing literature examines several approaches to co-ordinate the interdependencies between electric and natural gas systems. Zlotnik *et al*. [7] quantify the benefits that various levels of co-ordination between the two systems bring. Toledo *et al*. [8] investigate the impact of natural gas prices on operational costs of power systems. He *et al*. [9] implement a distributed day-ahead dispatch framework for operating the two systems. Other works examine co-ordination within a market-equilibrium framework. Khazeni *et al*. [10] develop a market-equilibrium model wherein profit-maximizing electricity and natural gas retailers are upper-level players that are followed by cost-minimizing lower-level retail customers. Wang *et al*. [11] develop an equilibrium model for strategic producers that participate in integrated electricity and natural gas markets. Ji and Huang [12] propose a bi-level model, where the upper level maximizes the profits of the market participants, while the lower level represents the independent clearing of interdependent electricity and natural gas markets. Wang *et al*. [13] study a coupled electricity and natural gas distribution market with bilateral energy trading. An equilibrium of these coupled markets is identified by a best-response decomposition algorithm.

The premise that underlies the co-ordination of the two systems within a market-equilibrium framework is that there is sufficient information exchanged between them. Thus, an outstanding question, which our work addresses, is the extent to which co-ordination can be achieved with limited information exchange. Some works that study the co-ordination of electricity and natural gas systems through a market framework [12], [13] employ algorithms that are sensitive to the initial point that is chosen [14]. Thus, a second gap in the existing literature that we address is to develop an approach that is not iterative and does not rely on the choice of an initial point.

Building off of these two gaps in the existing literature, we study the problem of co-ordinating the day-ahead operation of electric and natural gas systems with limited information-exchange between them. More specifically, the electric and natural gas systems operate independently, under perfectly competitive market structures, to minimize their respective operational costs. The operations of the two systems are interrelated, however, due to natural gas-fired units. Thus, the two systems must achieve an operational equilibrium, from which neither has a cost-reducing deviation. Our work develops a comprehensive approach to deriving such operational equilibria. The electric power system is represented using a DC load-flow model. A second-order-cone (SOC) relaxation of a natural gas-flow model that captures line-pack is used to represent the natural gas system [13], [15]. This SOC relaxation is enhanced by including convex envelopes [16]. Because these models are, respectively, linear and SOC problems, we can find a market equilibrium by using their Karush-Kuhn-Tucker (KKT) conditions [17]. This method is not dependent on or sensitive to the choice of an initial point in finding an equilibrium. Using this modeling framework, we examine the impacts on the operations of the two systems of having different levels of temporal and spatial granularity in communicating natural gas demands and prices between them. Our work is somewhat related to that of Gil *et al*. [18], who study the problem of co-ordinating the operation of separate electricity and natural gas departments within an integrated firm that operates in both markets. Their work is related to ours, insomuch as they examine the use of contract terms to co-ordinate operations of the two sides of the business, much as we examine the use of price signals to co-ordinate the operations of the two systems. Nevertheless, our work includes operational constraints of both electric and natural gas systems that are not considered by Gil *et al*.

In light of this existing literature, our work makes the following three contributions.

1) We characterize operational equilibria under different levels of temporal and spatial granularity in exchanging fuel-price information.
2) We develop a direct approach that includes the KKT conditions of both system-operational models to identify operational equilibria.
3) We use a case study, which is based on the Belgian system, to explore the impacts of different levels of granularity in exchanging information.

The remainder of this paper is organized as follows. Section II presents the two system models. Section III details the methodology that is employed to find solutions that are simultaneously optimal in the two system models and how different levels of temporal and spatial granularity in the information exchange are modeled. Section IV summarizes the results of our case study. Section V concludes.

II. System Models

We begin this section with the formulation of the natural gas-operational model and its convexification. We then formulate the power system-operational model.

A. Natural Gas System-Operational Model

The natural gas-operational model is formulated as [19]:

$$\min_{\Xi_{\mathrm{G}}} \sum_{t\in T, m\in\mathbb{N}, w\in\Psi_m^S} [C_{S,w}F_{S,w,t} + C^G\cdot(F_{L,m,t}-F^D_{L,m,t})] \tag{1}$$

$$\text{s.t. } F^D_{L,m,t} + \sum_{k\in\mathbb{C}(m)}(\tau_{k,t}+F_{C,k,t}) + \sum_{v\in\Psi_m^G}\eta_v P_{G,v,t} + \sum_{n\in\mathbb{G}(m)} F_{m,n,t} = \sum_{w\in\Psi_m^S} F_{S,w,t}; \forall m\in\mathbb{N}; t\in T \tag{2}$$

$$\bar{F}_{m,n,t} = (F_{m,n,t}-F_{n,m,t})/2; \forall m,n\in\mathbb{N}; t\in T \tag{3}$$

$$\bar{F}^2_{m,n,t}/W^2_{m,n} = \pi^2_{m,t}-\pi^2_{n,t}; \forall m,n\in\mathbb{N}; t\in T \tag{4}$$

$$F_{m,n,t}+F_{n,m,t} = L_{m,n,t}-L_{m,n,t-1}; \quad \forall m,n\in\mathbb{N}; t\in T \tag{5}$$

$$L_{m,n,t} = K_{m,n}\cdot(\pi_{m,t}+\pi_{n,t})/2; \forall m,n\in\mathbb{N}; t\in T \tag{6}$$

$$\tau_{k,t} = \vartheta_k F_{C,k,t}; \forall m\in\mathbb{N}; k\in\mathbb{C}(m); t\in T \tag{7}$$

$$\rho_k^{\min}\pi^{\text{in}}_{k,t} \le \pi^{\text{out}}_{k,t} \le \rho_k^{\max}\pi^{\text{in}}_{k,t}; \quad \forall m\in\mathbb{N}; k\in\mathbb{C}(m); t\in T \tag{8}$$

$$0\le F_{C,k,t}\le F^{\max}_{C,k}; \forall m\in\mathbb{N}; k\in\mathbb{C}(m); t\in T \tag{9}$$

$$F^{\min}_{S,w}\le F_{S,w,t}\le F^{\max}_{S,w}; \forall m\in\mathbb{N}; w\in\Psi^S_m; t\in T \tag{10}$$

$$-F^{\text{ramp}}_{S,w}\le F_{S,w,t}-F_{S,w,t-1}\le F^{\text{ramp}}_{S,w}; \quad \forall m\in\mathbb{N}; w\in\Psi^S_m; t\in T \tag{11}$$

$$\pi^{\min}_m\le\pi_{m,t}\le\pi^{\max}_m; \forall m\in\mathbb{N}; t\in T \tag{12}$$

$$\sum_{m,n\in\mathbb{N}} L_{m,n,|T|}\ge L_{\min}; \tag{13}$$

$$0\le F^D_{L,m,t}\le F_{L,m,t}; \forall m\in\mathbb{N}; t\in T; \tag{14}$$

where $\Xi_{\mathrm{G}} = \left\{F_{C,k,t}, F^D_{L,m,t}, F_{m,n,t}, \bar{F}_{m,n,t}, F_{S,w,t}, L_{m,n,t}, \pi^{\text{in}}_{k,t}, \pi^{\text{out}}_{k,t}, \pi_{m,t}, \tau_{k,t}\right\}$ is the variable set.

Objective function (1) computes the cost of operating the natural gas system. The first term in the objective function gives the cost of natural gas supply while the second is the cost of any curtailed non-generation-related natural gas demand. Constraints (2) impose hourly nodal natural gas balance between non-generation-related natural gas demand, compressor demand, flows through compressors, generation-related natural gas demand, natural gas flow through pipelines, and production from natural gas sources. Constraints (3) compute the average hourly natural gas flow in each pipeline in terms of the natural gas flow in each direction in the pipeline. Constraints (4) relate the hourly average natural gas flow in each pipeline to the difference between the squared pressures at the two ends of the pipe. We assume here that the direction of natural gas flows are known *a priori*, meaning that $\bar{F}_{m,n,t}\ge 0$. This is a reasonable assumption for day-ahead operations [20]. Constraints (5) compute the change in line-pack on each pipeline between hours t and $(t-1)$ and relate it to the flows on the pipeline. Constraints (6) give the linear relationship between the hourly line-pack in each pipeline and the average between the natural gas pressures at the two ends of the pipe. Constraints (5) and (6) imply that decreased nodal pressure results in a lower gas line-pack (*i.e.*, $L_{m,n,t} < L_{m,n,t-1}$), because additional natural gas from the line-pack is injected into the network (*i.e.*, $F_{m,n,t}+F_{n,m,t}>0$). Constraints (7) compute the hourly consumption of fuel of each compressor, which is simplified as a fixed percentage (typically between 3% and 5%) of the transported natural gas flow [19], [21]. Constraints (8) impose minimum and maximum compression ratios on the compressors while Constraints (9) enforce non-negativity and the transportation limit of the natural gas compressors. Constraints (10) and (11) impose production and ramping limits on the natural gas suppliers, respectively. Constraints (12) impose nodal pressure limits. Constraint (13) imposes a minimum line-pack over the entire system in the final period of the optimization horizon. Constraints (14) limit the amount of non-generation-related natural gas demand that is served to be non-negative and no greater than the corresponding nodal demand.

B. Convexification of Natural Gas-System Operational Model

Model (1)–(14) is non-convex due to (4), which can be equivalently written as:

$$\bar{F}^2_{m,n,t}/W^2_{m,n}\le\pi^2_{m,t}-\pi^2_{n,t}; \forall m,n\in\mathbb{N}; t\in T; \tag{15}$$

and:

$$\bar{F}^2_{m,n,t}/W^2_{m,n}\ge\pi^2_{m,t}-\pi^2_{n,t}; \forall m,n\in\mathbb{N}; t\in T. \tag{16}$$

Inequalities (15) are convex SOC constraints while (16) are non-convex. We can convexify the latter using convex envelopes [22] by first creating four sets of auxiliary variables, $a_{m,n,t}$, $b_{m,n,t}$, $\kappa_{m,n,t}$, and $\xi_{m,n,t}$ $\forall m,n\in\mathbb{N}; t\in T$. The variables, $\kappa_{m,n,t}$ and $\xi_{m,n,t}$, approximate $\bar{F}^2_{m,n,t}$ and $\pi^2_{m,t}-\pi^2_{n,t}$, respectively. With these variables, the convexification of (16) for all $m,n\in\mathbb{N}$ and $t\in T$ is given by:

$$a_{m,n,t} = \pi_{m,t}+\pi_{n,t}; \tag{17}$$

$$b_{m,n,t} = \pi_{m,t}-\pi_{n,t}; \tag{18}$$

$$\xi_{m,n,t}\ge a^{\min}_{m,n,t}b_{m,n,t}+b^{\min}_{m,n,t}a_{m,n,t}-a^{\min}_{m,n,t}b^{\min}_{m,n,t}; \tag{19}$$

$$\xi_{m,n,t}\ge a^{\max}_{m,n,t}b_{m,n,t}+b^{\max}_{m,n,t}a_{m,n,t}-a^{\max}_{m,n,t}b^{\max}_{m,n,t}; \tag{20}$$

$$\xi_{m,n,t}\le a^{\min}_{m,n,t}b_{m,n,t}+b^{\max}_{m,n,t}a_{m,n,t}-a^{\min}_{m,n,t}b^{\max}_{m,n,t}; \tag{21}$$

$$\xi_{m,n,t}\le a^{\max}_{m,n,t}b_{m,n,t}+b^{\min}_{m,n,t}a_{m,n,t}-a^{\max}_{m,n,t}b^{\min}_{m,n,t}; \tag{22}$$

$$\kappa_{m,n,t}\ge\bar{F}^2_{m,n,t}; \tag{23}$$

$$\kappa_{m,n,t}\le\left(F^{\max}_{m,n,t}+F^{\min}_{m,n,t}\right)\bar{F}_{m,n,t}-F^{\max}_{m,n,t}F^{\min}_{m,n,t}; \tag{24}$$

$$\kappa_{m,n,t}/W^2_{m,n}\ge\xi_{m,n,t}; \tag{25}$$

where $a^{\max}_{m,n,t}$, $a^{\min}_{m,n,t}$, $b^{\max}_{m,n,t}$, $b^{\min}_{m,n,t}$, $F^{\min}_{m,n,t}$, and $F^{\min}_{m,n,t}$ are fixed constants. Equalities (17) and (18) define $a_{m,n,t}$ and $b_{m,n,t}$ as the sum and differences between the nodal pressures at the two ends of the pipeline. By these definitions, we have that $a_{m,n,t}b_{m,n,t}=\pi^2_{m,t}-\pi^2_{n,t}$. Constraints (19)–(22) give the convex envelope that defines $\xi_{m,n,t}$ in terms of $a_{m,n,t}$ and $b_{m,n,t}$. Constraints (23) and (24) give the convex envelope that defines $\kappa_{m,n,t}$ in terms of $\bar{F}_{m,n,t}$. Finally, (25) relates $\kappa_{m,n,t}$ and $\xi_{m,n,t}$ to one another.

Fig. 1 shows the convexified bounds of $\pi^2_{m,t}-\pi^2_{n,t}$ for the special case in which $a_{m,n,t}=b_{m,n,t}$ (we illustrate this special case because (19)–(22) generally define hyperplanes,

which cannot be easily shown). Fig. 2 shows the convexified bounds of $\bar{F}^2_{m,n,t}$. With these auxiliary variables and constraints defined, the convexification of (1)–(14) is given by (1)–(3), (5)–(14), (15), and (17)–(25), which we refer to hereafter as the convexified natural gas system-operational model. The tightness of the convexified SOC natural gas flow model is demonstrated in our previous work [16]. Thus, it is not discussed here.

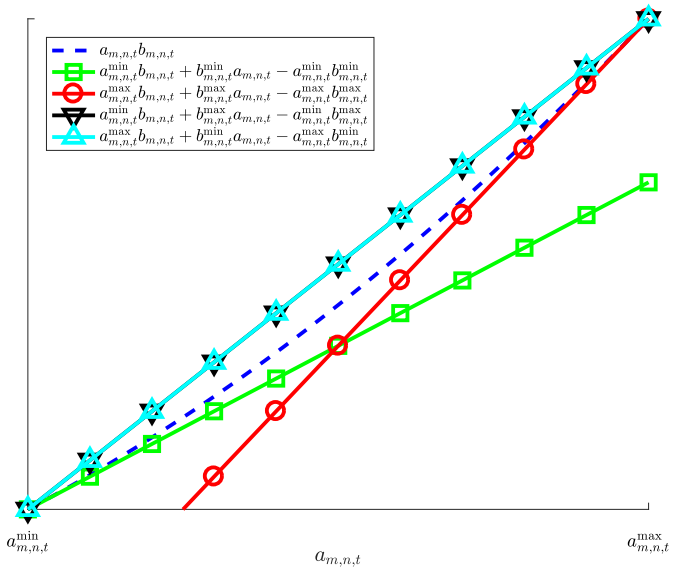

Fig. 1. Convexified approximation of $\pi^2_{m,t}-\pi^2_{n,t}$ that is given by (19)–(22) for the special case in which $a_{m,n,t}=b_{m,n,t}$.

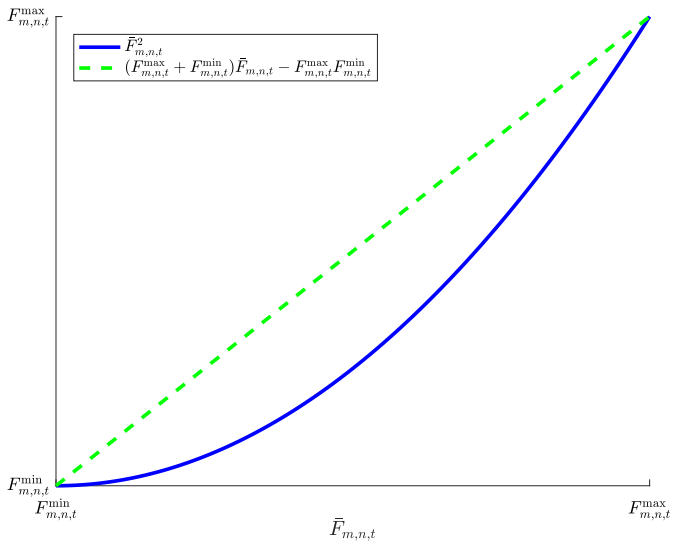

Fig. 2. Convexified approximation of $\bar{F}^2_{m,n,t}$ that is given by (23) and (24).

Because the convexified natural gas system-operational model is a convex SOC problem, the strong duality theorem applies if an appropriate constraint-qualification condition is satisfied [23]. We assume, hereafter, that such a condition is satisfied. As such, the problem is guaranteed to have well defined dual variables and we specifically define $u_{m,t}$ as the dual variable that is associated with node-m/hour-t Constraint (2). Intuitively, $u_{m,t}$ represents the node-m/hour-t natural gas locational marginal price (LMP) in \$/Mm^3.

C. Power System-Operational Model

The power system-operational problem is formulated as:

$$\min_{\Xi_{\mathrm{E}}} \sum_{t\in T}\Bigg[\sum_{m\in\mathbb{N},v\in\Psi^G_m}(C_{O,v}+\eta_v\zeta_{m,t})P_{G,v,t} + \sum_{v\in\Omega_R}C_{G,v}P_{G,v,t}+\sum_{i\in\mathbb{B}}C^E\cdot(P_{L,i,t}-P^D_{L,i,t})\Bigg] \tag{26}$$

$$\text{s.t.} \sum_{v\in\Theta^G_i}P_{G,v,t}=P^D_{L,i,t}+\sum_{j\in\mathbb{E}(i)}\sigma_{i,j}\cdot(\theta_{i,t}-\theta_{j,t}); \quad \forall i\in\mathbb{B};t\in T \tag{27}$$

$$P^{\min}_{G,v}\le P_{G,v,t}\le P^{\max}_{G,v};\forall v\in\Omega_G\cup\Omega_R;t\in T \tag{28}$$

$$-P^{\text{ramp}}_{G,v}\le P_{G,v,t}-P_{G,v,t-1}\le P^{\text{ramp}}_{G,v}; \quad \forall v\in\Omega_G\cup\Omega_R;t\in T \tag{29}$$

$$-P^{\max}_{i,j}\le b_{i,j}\cdot(\theta_{i,t}-\theta_{j,t})\le P^{\max}_{i,j}; \quad \forall i\in\mathbb{B};j\in\mathbb{E}(i);t\in T \tag{30}$$

$$\theta_{\text{REF},t}=0;t\in T \tag{31}$$

$$0\le P^D_{L,i,t}\le P_{L,i,t};\forall i\in\mathbb{B};t\in T; \tag{32}$$

where $\Xi_{\mathrm{E}}=\left\{P_{G,v,t},P^D_{L,i,t},\theta_{i,t}\right\}$ is the variable set.

Objective function (26) computes the power system-operations cost. The first two terms in the objective function represent the cost of operating natural gas-fired and non-natural gas-fired units, respectively, while the third computes load-curtailment cost. Constraints (27) impose hourly load balance on each bus. Constraints (28) and (29) impose capacity and ramping limits, respectively, on the generating units. Constraints (30) impose flow limits on the transmission lines while Constraints (31) fix the phase angle at the reference bus equal to zero in each hour. Constraints (32) limit the amount of load served at each bus to be non-negative and no greater than the corresponding hourly demand. We finally define $\lambda_{i,t}$ as the dual variable that is associated with hour bus-i/hour-t Constraint (27), which gives the hour bus-i/hour-t electric LMP in \$/p.u.

III. Solution Methodology

Although the two systems are modeled as being operated independently of one another, they are interdependent. This is because the dispatch of the power system impacts natural gas demands while the cost and availability of natural gas impact the power system dispatch. Thus, our goal is to obtain an operational equilibrium or a set of solutions to the two system problems that are simultaneously optimal in both (*i.e.*, neither system operator has a unilateral deviation from the operational equilibrium that reduces the cost of operating its system). Such an operational equilibrium can be found if the natural gas prices that are used to dispatch the electric power system perfectly reflect the corresponding true natural gas LMPs (*i.e.*, if $u_{m,t}=\zeta_{m,t}\ \forall m\in\mathbb{N}$ and $t\in T$). We begin in this section by first outlining the approach that we use to compute

numerically operational equilibria under such a perfect-pricing assumption. We then discuss how operational equilibria with different levels of spatial and temporal granularity in natural gas LMPs are computed.

A. Operational Equilibria Under Perfect-Price Assumption

To derive operational equilibria under the perfect-price assumption (and for notational ease), we begin by writing the convexified natural gas system-operational model in compact matrix form as:

$$\min_{r,s} \; e^\top r \tag{33}$$

$$\text{s.t.} \quad J_1 r + E_1 s - h_1 + D_1 y = 0; \qquad (u) \tag{34}$$

$$J_2 r + E_2 s - h_2 \leq 0; \qquad (\nu) \tag{35}$$

$$s_q \in \Delta; \qquad \forall q \in \Lambda; \quad (\omega_q) \tag{36}$$

where the dual-variable vector that is associated with each constraint appears in parentheses to its right. r and s are decision-variable vectors. More specifically, r contains the variables $F_{C,k,t}$, $F^D_{L,m,t}$, $F_{m,n,t}$, $F_{S,w,t}$, $L_{m,n,t}$, $\pi^{\text{in}}_{k,t}$, $\pi^{\text{out}}_{k,t}$, and $\tau_{k,t}$, while s contains the variables $\bar{F}_{m,n,t}$ and $\pi_{m,t}$. e, h_1, and h_2 are parameter vectors and J_1, J_2, E_1, E_2, and D_1 are parameter matrices. q represents the index of the cones and Λ represents the set of cones. Δ is a cone and $s_q \in \Delta$ means $s_{q,1} \geq \sqrt{s^2_{q,2} + s^2_{q,3} + \cdots + s^2_{q,d}}$, where d is the dimension of the vector, s_q. y is a vector of variables that are determined in the power system-operational model that directly impact the operation of the natural gas system (*i.e.*, the dispatch of the natural gas-fired units). Because the value of y is determined in the power system-operational model, it is considered a parameter vector in (33)–(36). The dual-variable vector, u, includes the natural gas LMPs, $u_{m,t} \forall m \in \mathbb{N}, t \in T$. However, u also includes dual variables that are associated with other equality constraints in the convexified natural gas system model.

We similarly write the power system-operational model in compact matrix form as:

$$\min_{x,y} \; c_1^\top x + c_2^\top y + \zeta^\top D_1 y \tag{37}$$

$$\text{s.t.} \quad A_1 x + B_1 y - g_1 = 0; \qquad (\lambda) \tag{38}$$

$$A_2 x + B_2 y - g_2 \leq 0; \qquad (\gamma) \tag{39}$$

where the dual-variable vector that is associated with each constraint is in parentheses to its right. x and y are decision-variable vectors, where x contains the variables $P_{G,v,t}$ (only for $v \in \Omega_R$), $P^D_{L,i,t}$, and $\theta_{i,t}$, and y contains the variables $P_{G,v,t}$ (only for $v \in \Omega_G$). y represents decision variables that directly impact the operation of the natural gas system (*i.e.*, the dispatch of natural gas-fired units). c_1, c_2, g_1, and g_2 are parameter vectors and A_1, A_2, B_1, B_2, and D_1 are parameter matrices. ζ is a vector that represents the cost of using natural gas in dispatching the electric power system.

Comparing (33)–(36) and (37)–(39) reveals two interrelationships in operating the two systems. First, y is a decision-variable vector in (37)–(39) but also appears in (34). Second, the natural gas-cost vector, ζ, which appears in (37) is related to the dual-variable vector, u, that is associated with (34). As such, the two problems cannot be solved independently of one another. This inability to solve the problems independently motivates our desire to obtain an operational equilibrium, which we do by simultaneously solving the necessary and sufficient KKT conditions of the two problems [14], [17]. The strong-duality theorem holds for the linear power system-operational model. Provided that Slater constraint-qualification conditions are satisfied, the strong-duality theorem also applies to the convexified SOC relaxation of the natural gas system-operational model [23].

The KKT conditions of (33)–(36) are:

$$e + J_1^\top u + J_2^\top \nu = 0; \tag{40}$$

$$E_1^\top u + E_2^\top \nu - \omega = 0; \tag{41}$$

$$J_1 r + E_1 s - h_1 + D_1 y = 0; \tag{42}$$

$$0 \leq \nu \perp J_2 r + E_2 s - h_2 \leq 0; \tag{43}$$

$$s_q, \omega_q \in \Delta; \forall q \in \Lambda; \tag{44}$$

$$\omega_q^\top s_q = 0; \forall q \in \Lambda. \tag{45}$$

Conditions (40) and (41) impose stationarity with respect to r and s, respectively. Condition (42) is the equality constraint of the original problem while (43) is the inequality constraint with complementary slackness. Condition (44) forces s to be within the cone, Δ, and imposes the same requirement on the dual-variable variable that is associated with the SOC constraint. Condition (45) imposes complementary slackness between s and ω.

The KKT conditions for (37)–(39) are:

$$c_1 + A_1^\top \lambda + A_2^\top \gamma = 0 \tag{46}$$

$$c_2 + D_1^\top \zeta + B_1^\top \lambda + B_2^\top \gamma = 0 \tag{47}$$

$$A_1 x + B_1 y - g_1 = 0 \tag{48}$$

$$0 \leq \gamma \perp A_2 x + B_2 y - g_2 \leq 0. \tag{49}$$

Conditions (46) and (47) impose stationarity with respect to x and y, respectively. Condition (48) is the equality constraint while Condition (49) is the inequality constraint with complementary slackness.

We can obtain an operational equilibrium by simultaneously solving (40)–(49) and the additional perfect-pricing condition:

$$\zeta_{m,t} = u_{m,t}, \forall m \in \mathbb{N}; t \in T. \tag{50}$$

However, these conditions include two types of non-convexities, which complicate their solution. First, the complementary-slackness requirements in (43) and (49) are non-convex, because, for instance, the complementary-slackness requirement in (43) can be written as:

$$\nu \cdot (J_2 r + E_2 s - h_2) = 0.$$

We use the method that is outlined by Fortuny-Amat and McCarl [24], which requires the use of binary variables, to linearize the complementary-slackness requirements in (43) and (49).

The second non-convexity arises from (45). We can linearize this by using the strong-duality condition for (33)–(36), which is:

$$e^\top r = -h_1^\top u + y^\top D_1^\top u - h_2^\top \nu + \sum_{q \in \Lambda} w_q^\top s_q. \tag{51}$$

Substituting this equality into (45) gives the equality:

$$e^\top r + h_1^\top u - y^\top D_1^\top u + h_2^\top \nu = 0. \quad (52)$$

This equality is non-convex because both y and u are variables when solving the full set of KKT conditions. Thus, $y^\top D_1^\top u$ is bilinear. We can linearize this term by using the strong-duality condition for (37)–(39) [17], which is:

$$c_1^\top x + c_2^\top y + \zeta^\top D_1 y = -g_1^\top \lambda - g_2^\top \gamma. \quad (53)$$

Substituting this condition and (50) into (52) gives:

$$e^\top r + h_1^\top u + c_1^\top x + c_2^\top y + g_1^\top \lambda + g_2^\top \gamma + h_2^\top \nu = 0. \quad (54)$$

Thus, taking these linearizations together, we can obtain an operational equilibrium by solving the mixed-integer SOC problem:

$$\min\ 1 \quad (55)$$

$$\text{s.t.}\ \ (40)\text{–}(44),\ (46)\text{–}(49),\ (50),\ (54) \quad (56)$$

where the complementary-slackness conditions in (43) and (49) are replaced by their linearizations using binary variables. The objective function of this problem is arbitrarily fixed equal to unity, while the constraints impose the convexified KKT conditions of the two problems and the perfect-pricing assumption.

A diagonalization algorithm is used to verify whether a solution that is provided by (55) and (56) is an equilibrium. This is because (55) and (56) only provide KKT points for the two system models, which may not necessarily be an equilibrium.

B. Operational Equilibria Under Different Price-Granularity Levels

The operational equilibria that are obtained from (55)–(56) assume perfect price-based co-ordination between the electric and natural gas systems. In practice, the two systems do not have this level of information exchange. Indeed, wholesale natural gas prices typically lack the spatial and temporal granularity of the natural gas LMPs that are given by u. As such, we develop a method of computing operational equilibria under different levels of price granularity. Doing so allows us to quantitatively analyze the value of using imperfect versus perfect natural gas LMPs to co-ordinate the operation of the two systems.

Modeling imperfect natural gas pricing requires replacing (50) with alternate conditions that define ζ as spatial or temporal averages of u.[1] Moreover, because the perfect-pricing assumption is relaxed, the linearization of (45) that yields (54) is no longer valid. Thus, we compute operational equilibria using a non-convex nonlinear optimization problem, in which the complementary-slackness conditions are not convexified.

[1]Because u is a dual-variable variable that is associated with all of the equality constraints in the natural gas-system operational model, it includes dual variables that are not natural gas LMPs. Thus, in actuality, we only replace (50) for values of u that correspond to the natural gas LMPs.

Specifically, we examine three cases. The first considers temporal averaging of the natural gas LMPs. In this case, (50) is replaced with:

$$\zeta_{m,t} = \frac{1}{|T|}\sum_{\iota\in T} u_{m,\iota}; \forall m \in \mathbb{N}; t \in T; \quad (57)$$

which defines $\zeta_{m,t}$ as the simple average (over the $|T|$ hours of the model horizon) of the true natural gas LMPs at node m. The second case considers spatial averaging of the natural gas LMPs, in which case (50) is replaced with:

$$\zeta_{m,t} = \sum_{\mu\in\mathbb{N}} F_{L,\mu,t} u_{\mu,t} / \sum_{\mu\in\mathbb{N}} F_{L,\mu,t}, \forall m \in \mathbb{N}; t \in T. \quad (58)$$

This defines $\zeta_{m,t}$ as the weighted (by the non-generation-related natural gas demands) average (over the nodes) of the true natural gas LMPs in hour t. The final case that we examine assumes combined temporal and spatial averaging of natural gas LMPs. In this case (50) is replaced with:

$$\zeta_{m,t} = \frac{1}{|T|}\sum_{\iota\in T}\left(\sum_{\mu\in\mathbb{N}} F_{L,\mu,\iota} u_{\mu,\iota} / \sum_{\mu\in\mathbb{N}} F_{L,\mu,\iota}\right), \quad \forall m \in \mathbb{N}; t \in T. \quad (59)$$

In all three of these cases, an operational equilibrium is obtained by using primal/dual conditions for each of (33)–(36) and (37)–(39). The primal/dual conditions for the former are (40)–(42), (44), (45), and (51) while those of the latter are (46)–(48) and (53). Thus, the operational equilibria under imperfect pricing are obtained by solving:

$$\min\ 1 \quad (60)$$

$$\text{s.t.}\ \ (40)\text{–}(42),\ (44)\text{–}(48),\ (51),\ (53), \quad (61)$$

and one of (57), (58), or (59).

C. Value of Perfect Pricing

Once we obtain operational equilibria under the four pricing assumptions (*i.e.*, perfect, temporal averaging, spatial averaging, and combined averaging), we can compare the true combined cost of operating the natural gas and electric power systems. Comparing this cost in the three averaging cases to the perfect-pricing case gives a measure of the value of perfect pricing (VPP). To do this, we note that the *actual* cost of operating the natural gas system is given by (1), while the actual cost of operating the power system is given by:

$$\sum_{t\in T}\left[\sum_{m\in\mathbb{N},v\in\Psi_m^G} C_{O,v} P_{G,v,t} + \sum_{v\in\Omega_R} C_{G,v} P_{G,v,t} + \sum_{i\in\mathbb{B}} C^E \cdot (P_{L,i,t} - P_{L,i,t}^D)\right]. \quad (62)$$

This cost is equivalent to (26), except that the $\eta_v \zeta_{m,t} P_{G,v,t}$ term is removed. This is because the cost of supplying fuel to natural gas-fired generating units is implicitly accounted for in computing the cost of operating the natural gas system in (1). Thus, including $\eta_v \zeta_{m,t} P_{G,v,t}$ in (62) would double-count this cost. With this definition, we can compute the cost

of operating the two systems under the four sets of operational equilibria by substituting the values of $F^D_{L,m,t}$, $F_{S,w,t}$, $P_{G,v,t}$, and $P^D_{L,i,t}$ that are obtained under each pricing assumption into (1) and (62), respectively. The VPP, which is measured as a percentage, is given by:

$$\frac{C^{\mathrm{I}}_{\mathrm{EG}} - C^{\mathrm{P}}_{\mathrm{EG}}}{C^{\mathrm{P}}_{\mathrm{EG}}} \cdot 100, \tag{63}$$

where $C^{\mathrm{P}}_{\mathrm{EG}}$ and $C^{\mathrm{I}}_{\mathrm{EG}}$ represent the sum of (1) and (62) under perfect- and imperfect-pricing cases, respectively.

IV. Case Study

This section illustrates the performance of the proposed model using a case study that is based on the Belgian electric and natural gas systems. Fig. 3 shows the topology of the 24-bus power system[2] and 20-node natural gas system [19] that we study. The natural gas-fired units that are at buses 2, 3, 6, 8, 16, 15 and 22 are connected to natural gas nodes 4, 3, 4, 4, 6, 11, and 13, respectively. The generating units have an installed capacity of 13.95 GW, with natural gas-fired units contributing 30.2% of this total. Fig. 4 summarizes the diurnal electricity and non-generation-related natural gas demands that are used in the case study. Electricity demands are obtained from the same source that provides the network data. Non-generation-related natural gas demands are obtained from the work of [19] and scaled based on actual daily natural gas consumption data.[3] All of the case study data are provided in an online supplement.[4]

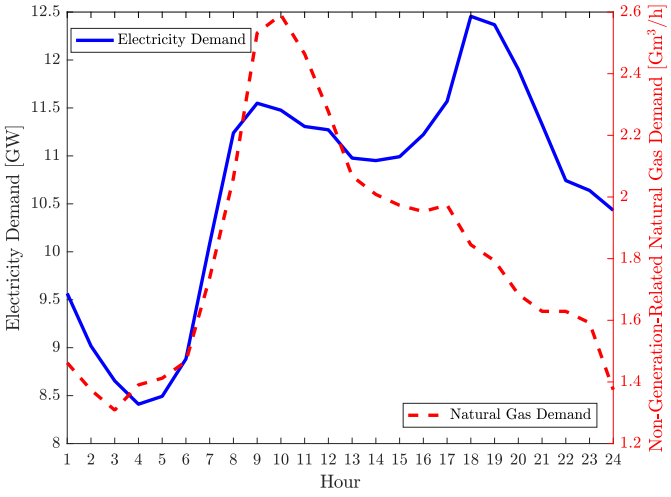

Fig. 4. Diurnal electricity and non-generation-related natural gas demands.

Both the perfect- and imperfect-pricing operational-equilibrium models are programmed using GAMS 24.7. The former is solved using CPLEX 12.6.3.0.2 while the latter is solved using IPOPT 3.12. The computations are carried out on a computer with a 2.5 GHz Intel Core process and 8 GB of memory. Modeling the perfect-pricing case requires the selection of big-M parameters that are used to linearize the complementary-slackness conditions. The big-M values for primal constraints are determined based on induced bounds. The big-M values for Lagrange multipliers are determined based on dual-variable values that are obtained from solving each of the convexified natural gas system-operational and power system-operational models on their own.

Table I summarizes the system-operations costs in the perfect- and three imperfect-pricing cases, as well as the VPPs. As expected, imperfect pricing results in slightly higher system-operations costs, although the breakdown of the cost increases differs between the four cases.

TABLE I
System-Operations Costs [$ Million] and VPPs [%]

Pricing Case	System-Operations Costs Natural Gas	Electric	Total	VPP
Perfect	5.529	4.384	9.913	n/a
Temporal Average	5.432	4.529	9.961	0.483
Spatial Average	5.796	4.163	9.959	0.477
Combined Average	5.609	4.359	9.968	0.558

Figs. 5 and 6 show hourly load-weighted natural gas and electric LMPs. Contrasting the cases of perfect pricing and temporal averaging, we see that the latter results in higher natural gas LMPs during peak periods (hours 8–15) and lower prices during off-peak periods (the remaining hours). These price impacts result in noticeably lower on-peak and slightly higher off-peak electric LMPs and a less volatile diurnal electric LMP profile with temporal averaging. The reduced volatility is due to the marginal generation cost of each natural gas-fired unit being constant over the day. Fig. 7 shows hourly total natural gas-fired production in the four pricing courses. The figures shows that temporal, spatial, and combined averaging of natural gas prices result in distorted dispatch decisions relative to the perfect-pricing case.

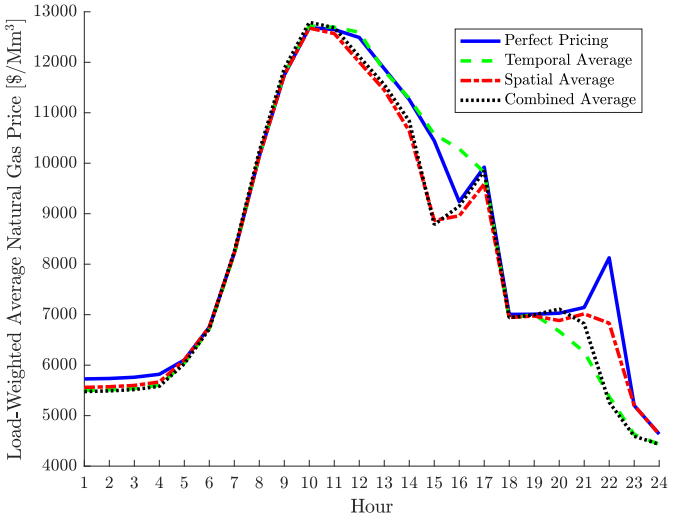

Fig. 5. Load-weighted natural gas LMPs with perfect, temporal, spatial, and combined averaging.

Fig. 8 shows the range of natural gas LMPs at nodes that are connected to natural gas-fired generators with perfect

[2]https://doi.org/10.5281/zenodo.999150
[3]https://www.quandl.com/data/BP/GAS_CONSUM_D_BEL
[4]https://doi.org/10.6084/m9.figshare.8848553.v1

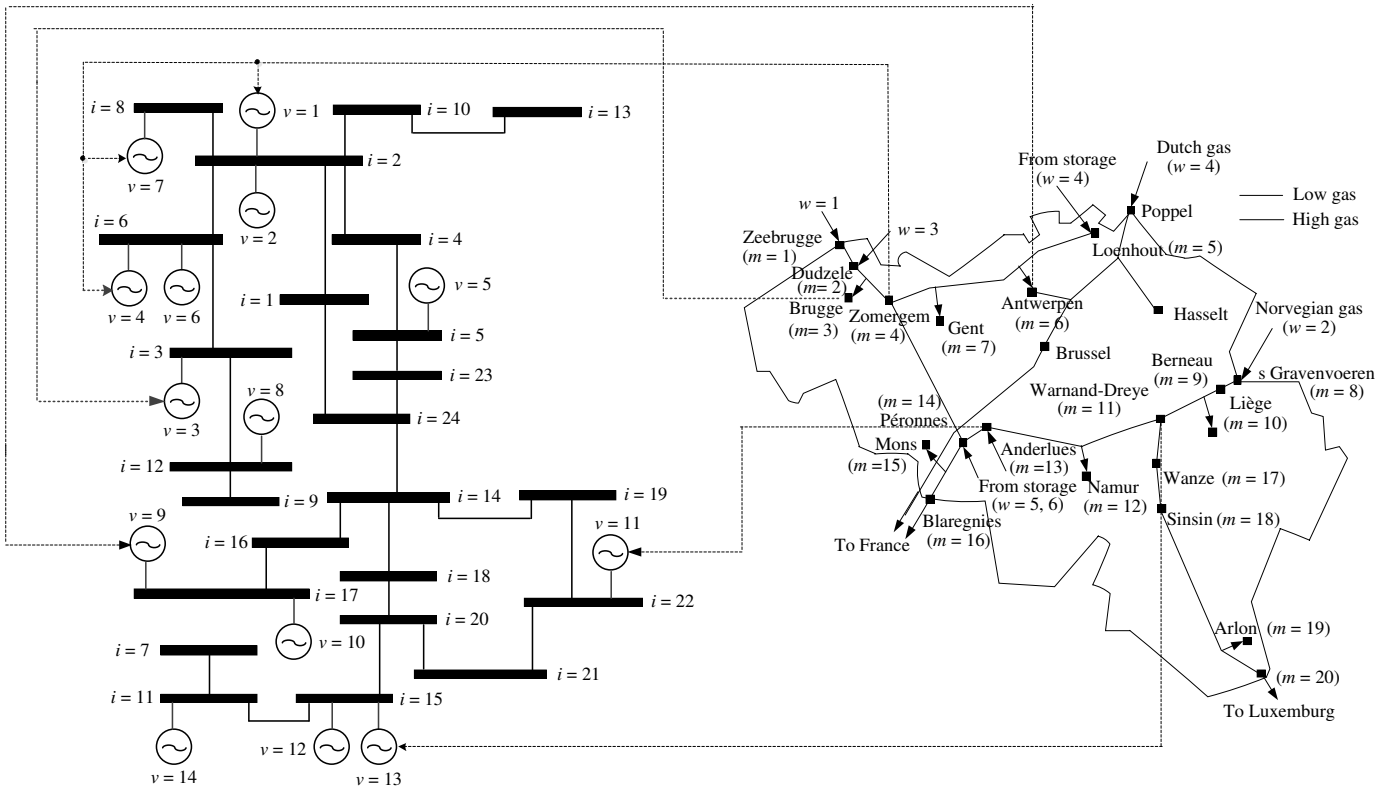

Fig. 3. Belgian-based 24-bus power system and 20-node natural gas system.

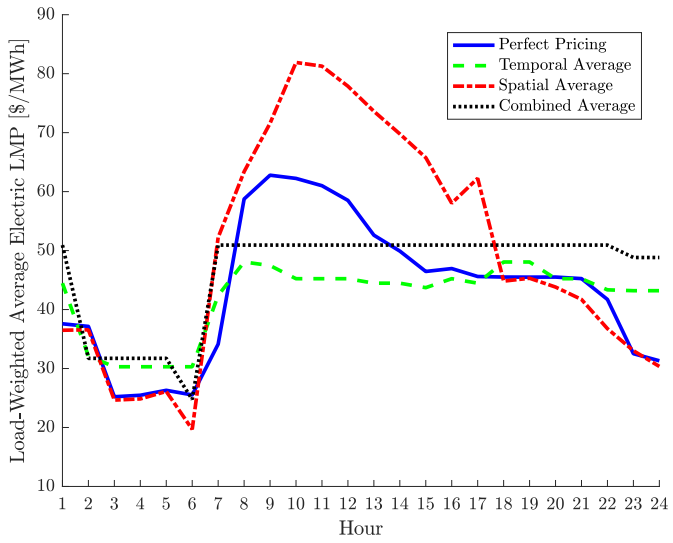

Fig. 6. Load-weighted electric LMPs with perfect, temporal, spatial, and combined averaging.

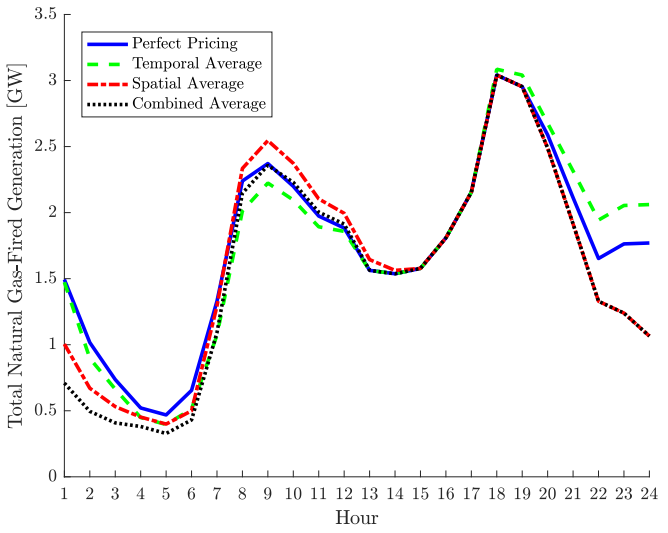

Fig. 7. Total natural-gas fired production in each hour with perfect, temporal, spatial, and combined averaging.

pricing. It also shows the values of ζ that are obtained from spatial averaging. The figure shows that in many hours, spatial averaging increases the fuel cost of natural gas-fired units. This is largely because natural gas-fired units in the Belgian system are connected to nodes that are relatively unconstrained from a fuel-supply perspective. Thus, natural gas LMPs at nodes to which natural gas-fired units are connected are typically lower than those at other nodes. As such, spatial averaging results in much higher fuel prices, especially during on-peak periods (*e.g.*, hours 9–12). These higher fuel prices yield higher electric LMPs, particularly during the on-peak period, as is shown in Fig. 6. Interestingly, Fig. 5 shows that in some hours spatial averaging results in lower natural gas LMPs compared to perfect pricing. This is because spatial averaging results in natural gas-fired generators having higher operating costs, which reduces their use (thereby reducing the *actual* cost of supplying natural gas). These higher fuel costs with spatial averaging also yield the increased power system-operational

costs and lower natural gas system-operational costs that are summarized in Table I. If the natural gas system is highly congested, natural gas LMPs may significantly differ between nodes. In such a case, the fuel costs of natural-gas fired units that are provided by spatial averaging deviate from their 'true' values. Hence, in such a case spatially averaged natural gas prices are undesirable for system operations.

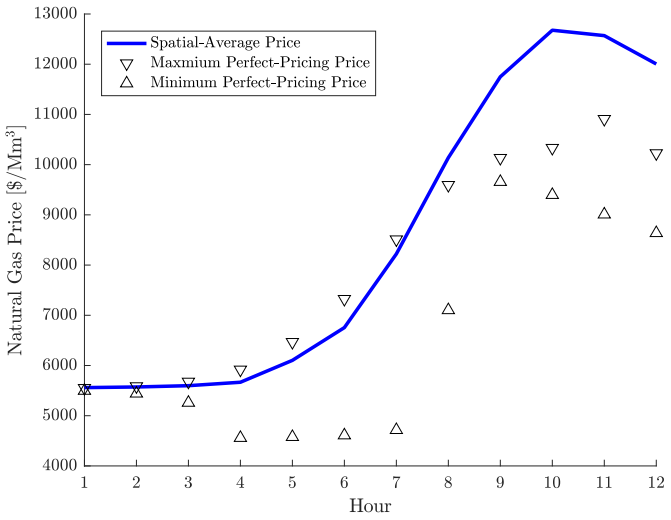

Fig. 8. Range of natural gas LMPs at nodes with natural gas-fired generators in perfect-pricing case and spatial-average prices.

Table I shows that combined averaging yields a higher VPP than either temporal or spatial averaging do on their own, indicating that insufficient coordination between the two systems results in higher operational costs. However, the combined effect is less than the sum of the effects of temporal and spatial averaging on their own. This suggests subadditive efficiency losses from both temporal and spatial averaging together. Fig. 5 shows that combined averaging yields lower natural gas LMPs compared to perfect pricing. This is due largely to the same effect that yields lower natural gas LMPs with spatial averaging—combined averaging increases the operating cost of natural gas-fired units, reducing their use and natural gas consumption. Fig. 6 shows that combined averaging yields higher electric LMPs during hours 1, 3–5, 7, and 14–24 compared to perfect pricing. This is due to the same effect that causes higher electric LMPs with temporal averaging—the operating costs of natural gas-fired units are increased in off-peak hours relative to perfect pricing. As with temporal averaging, combined averaging yields lower on-peak electric LMPs relative to the LMPs that are obtained with perfect pricing (*i.e.*, because the operating costs of natural gas-fired units are decreased in on-peak hours relative to perfect pricing). Combined averaging yields the same electric LMPs across hours 7–22, which is due to all of the natural gas-fired units having the same fuel costs across all of the hours of the day.

The perfect- and imperfect-pricing operational equilibrium models require about 2310 s and 190 s, respectively, of wall-clock time to solve.

V. Conclusions

This paper proposes an operational-equilibrium model for the independent but interrelated day-ahead operation of electric and natural gas systems. We develop a direct approach, which relies upon the optimality conditions of both system-operational models to compute operational equilibria between the two systems. We investigate the impacts of different levels of both temporal and spatial granularity in communicating fuel-price information between the two systems on their operations. Computational results, using a case study that is based on the Belgian electric power and natural gas systems, indicate that exact information interchange between the two systems is desirable to co-ordinate their operations most efficiently. We show that temporal, spatial, and combined averaging of natural gas prices have spillover effects on electric LMPs. The natural gas system-operational model that we use is a simplification, as many natural gas system are decentralized and involve more than one operator. Nevertheless, our analysis provides a formative analysis of the benefits of tighter co-ordination between the two systems using market-based mechanisms.

Most wholesale natural gas markets employ pricing that is akin to combined averaging. This is because these markets have only a handful of locational pricing hubs and delivery points. Moreover, many wholesale markets set a single daily price for natural gas. Our results show that these pricing practices introduce overall efficiency losses to the whole system (*i.e.*, considering both systems together). Moreover, there are mixed impacts of combined averaging on the efficiency and cost of operating the two systems. In our case study, combined averaging increases the cost of operating the natural gas system relative to perfect pricing. This is largely due to combined averaging decreasing the perceived cost of operating the natural gas-fired generating fleet compared to perfect pricing. Given these findings, operators of natural gas systems may have incentives to implement more granular pricing practices, to reduce the costs of operating their own systems.

Acknowledgment

The authors thank the editors and six reviewers for useful comments and suggestions. The third author thanks A. Sorooshian for helpful suggestions, comments, and conversations.

References

[1] T. Ding, Y. Hu, and Z. Bie, "Multi-Stage Stochastic Programming with Nonanticipativity Constraints for Expansion of Combined Power and Natural Gas Systems," *IEEE Transactions on Power Systems*, vol. 33, pp. 317–328, January 2018.

[2] R. Bent, S. Blumsack, P. Van Hentenryck, C. Borraz-Sánchez, and M. Shahriari, "Joint Electricity and Natural Gas Transmission Planning With Endogenous Market Feedbacks," *IEEE Transactions on Power Systems*, vol. 33, pp. 6397–6409, November 2018.

[3] S. Chen, Z. Wei, G. Sun, K. W. Cheung, and Y. Sun, "Multi-Linear Probabilistic Energy Flow Analysis of Integrated Electrical and Natural-Gas Systems," *IEEE Transactions on Power Systems*, vol. 32, pp. 1970–1979, May 2017.

[4] B. Zhao, A. J. Conejo, and R. Sioshansi, "Unit Commitment Under Gas-Supply Uncertainty and Gas-Price Variability," *IEEE Transactions on Power Systems*, vol. 32, pp. 2394–2405, May 2017.

[5] E. C. Portante, J. A. Kavicky, B. A. Craig, L. E. Talaber, and S. M. Folga, "Modeling Electric Power and Natural Gas System Interdependencies," *Journal of Infrastructure Systems*, vol. 23, p. 04017035, December 2017.
[6] C. Shao, X. Wang, M. Shahidehpour, X. Wang, and B. Wang, "An MILP-Based Optimal Power Flow in Multicarrier Energy Systems," *IEEE Transactions on Sustainable Energy*, vol. 8, pp. 239–248, January 2017.
[7] A. Zlotnik, L. Roald, S. Backhaus, M. Chertkov, and G. Andersson, "Coordinated Scheduling for Interdependent Electric Power and Natural Gas Infrastructures," *IEEE Transactions on Power Systems*, vol. 32, pp. 600–610, January 2017.
[8] F. Toledo, E. Sauma, and S. Jerardino, "Energy Cost Distortion Due to Ignoring Natural Gas Network Limitations in the Scheduling of Hydrothermal Power Systems," *IEEE Transactions on Power Systems*, vol. 31, pp. 3785–3793, September 2016.
[9] C. He, L. Wu, T. Liu, and M. Shahidehpour, "Robust Co-Optimization Scheduling of Electricity and Natural Gas Systems via ADMM," *IEEE Transactions on Sustainable Energy*, vol. 8, pp. 658–670, November 2017.
[10] S. Khazeni, A. Sheikhi, M. Rayiati, S. Soleymani, and A. M. Ranjbar, "Retail Market Equilibrium in Multicarrier Energy Systems: A Game Theoretical Approach," *IEEE Systems Journal*, 2019, in press.
[11] C. Wang, W. Wei, J. Wang, F. Liu, and S. Mei, "Strategic Offering and Equilibrium in Coupled Gas and Electricity Markets," *IEEE Transactions on Power Systems*, vol. 33, pp. 290–306, January 2018.
[12] Z. Ji and X. Huang, "Day-Ahead Schedule and Equilibrium for the Coupled Electricity and Natural Gas Markets," *IEEE Access*, vol. 6, pp. 27 530–27 540, 2018.
[13] C. Wang, W. Wei, J. Wang, L. Wu, and Y. Liang, "Equilibrium of Interdependent Gas and Electricity Markets with Marginal Price Based Bilateral Energy Trading," *IEEE Transactions on Power Systems*, vol. 33, pp. 4854–4867, September 2018.
[14] S. A. Gabriel, A. J. Conejo, J. D. Fuller, B. F. Hobbs, and C. Ruiz, Eds., *Complementarity Modeling in Energy Markets*, ser. International Series in Operations Research & Management Science. New York, New York: Springer-Verlag, 2013, vol. 189.
[15] C. B. Sánchez, R. Bent, S. Backhaus, S. Blumsack, H. Hijazi, and P. van Hentenryck, "Convex Optimization for Joint Expansion Planning of Natural Gas and Power Systems," in *49th Hawaii International Conference on System Sciences*, Koloa, Hawaii, 5-8 January 2016, pp. 2536–2545.
[16] S. Chen, A. J. Conejo, R. Sioshansi, and Z. Wei, "Unit Commitment with an Enhanced Natural Gas-Flow Model," *IEEE Transactions on Power Systems*, 2019, in press.
[17] C. Ruiz, A. J. Conejo, and Y. Smeers, "Equilibria in an Oligopolistic Electricity Pool With Stepwise Offer Curves," *IEEE Transactions on Power Systems*, vol. 27, pp. 752–761, May 2012.
[18] M. Gil, P. Dueñas, and J. Reneses, "Electricity and Natural Gas Interdependency: Comparison of Two Methodologies for Coupling Large Market Models Within the European Regulatory Framework," *IEEE Transactions on Power Systems*, vol. 31, pp. 361–369, January 2016.
[19] C. M. Correa-Posada and P. Sánchez-Martín, "Integrated Power and Natural Gas Model for Energy Adequacy in Short-Term Operation," *IEEE Transactions on Power Systems*, vol. 30, pp. 3347–3355, November 2015.
[20] O. Massol and A. Banal-Estañol, "Market Power and Spatial Arbitrage between Interconnected Gas Hubs," *The Energy Journal*, vol. 39, pp. 67–95, 2018.
[21] J. Qiu, H. Yang, Z. Y. Dong, J. H. Zhao, K. Meng, F. J. Luo, and K. P. Wong, "A Linear Programming Approach to Expansion Co-Planning in Gas and Electricity Markets," *IEEE Transactions on Power Systems*, vol. 31, pp. 3594–3606, September 2016.
[22] C. Coffrin, H. L. Hijazi, and P. V. Hentenryck, "The QC Relaxation: A Theoretical and Computational Study on Optimal Power Flow," *IEEE Transactions on Power Systems*, vol. 31, pp. 3008–3018, July 2016.
[23] A. Ben-Tal and A. Nemirovski, *Lectures on Modern Convex Optimization: Analysis, Algorithms, and Engineering Applications*, ser. MOS-SIAM Series on Optimization. Philadelphia, Pennsylvania: Society for Industrial and Applied Mathematics, 2001.
[24] J. Fortuny-Amat and B. McCarl, "A Representation and Economic Interpretation of a Two-Level Programming Problem," *The Journal of the Operational Research Society*, vol. 32, pp. 783–792, September 1981.

Sheng Chen (M'19) received his B.S. and Ph.D. degrees from the College of Energy and Electrical Engineering, Hohai University, Nanjing, China, in 2014 and 2019, respectively. From January 2018 to January 2019 he was a visiting scholar at The Ohio State University, Columbus, OH.

He is currently an associate professor in the College of Energy and Electrical Engineering, Hohai University, Nanjing, China. His research interests include integrated energy systems, operations research, and electricity markets.

Antonio J. Conejo (F'04) received the M.S. degree from the Massachusetts Institute of Technology, Cambridge, MA, in 1987, and the Ph.D. degree from the Royal Institute of Technology, Stockholm, Sweden, in 1990.

He is currently a professor in the Department of Integrated Systems Engineering and the Department of Electrical and Computer Engineering, The Ohio State University, Columbus, OH. His research interests include control, operations, planning, economics and regulation of electric energy systems, as well as statistics and optimization theory and its applications.

Ramteen Sioshansi (M'11–SM'12) holds the B.A. degree in economics and applied mathematics and the M.S. and Ph.D. degrees in industrial engineering and operations research from the University of California, Berkeley, and an M.Sc. in econometrics and mathematical economics from The London School of Economics and Political Science.

He is a professor in the Department of Integrated Systems Engineering at The Ohio State University, Columbus, OH. His research focuses on renewable and sustainable energy system analysis and the design of restructured competitive electricity markets.

Zhinong Wei received the B.S. degree from Hefei University of Technology, Hefei, China, in 1984, the M.S. degree from Southeast University, Nanjing, China, in 1987, and the Ph.D. degree from Hohai University, Nanjing, China, in 2004.

He is now a professor of electrical engineering with the College of Energy and Electrical Engineering, Hohai University, Nanjing, China. His research interests include integrated energy systems, power system state estimation, smart distribution systems, and integration of distributed generation into electric power systems.